

Preparation of Superparamagnetic Fe₃O₄ Nanoparticles from Iron Sand Mediated by Soft Template and Their Performance as Antibacterial Agent

A. Taufiq^{1*}, A. F. Muyasaroh¹, S. Sunaryono¹, H. Susanto², N. Hidayat¹, N. Mufti¹,
E. Suarsini², A. Hidayat¹, A. Okazawa³, T. Ishida⁴, and D. Darminto⁵

¹Department of Physics, Faculty of Mathematics and Natural Sciences, Universitas Negeri Malang,
Jl. Semarang 5, Malang 65145, Indonesia

²Department of Biology, Faculty of Mathematics and Natural Sciences, Universitas Negeri Malang,
Jl. Semarang 5, Malang 65145, Indonesia

³Department of Basic Science, the University of Tokyo, Komaba, Meguro-ku, Tokyo 153-8902, Japan

⁴Department of Engineering Science, the University of Electro-Communications, Chofu, Tokyo 182-8585, Japan

⁵Department of Physics, Faculty of Science, Institut Teknologi Sepuluh Nopember, Jl. A. R. Hakim, Surabaya 60111, Indonesia

(Received 3 February 2018, Received in final form 4 July 2018, Accepted 15 July 2018)

In this work, the soft-template technique was employed in preparing the superparamagnetic Fe₃O₄ nanoparticles from natural iron sand. A series of the Fe₃O₄ nanoparticles formed spinel crystal structure with the particle size in the range of 1.9 to 6.6 nm which was varied by diethylamine concentration as the template. All samples had the functional groups of Fe³⁺-O²⁻, Fe²⁺-O²⁻ and OH and exhibited the superparamagnetic character. The antibacterial activity of the Fe₃O₄ nanoparticles showed a significant outcome to pathogen growth rate. Pre-administration of bacterial stock solution (*E. coli* and *B. subtilis*) with magnetite significantly reduced the colony formation compared to control group. In particular, for Gram-negative bacteria growth rate, pretreatment with magnetite declined the colony formation considerably compared to placebo and positive control group. Also, in line with Gram-negative bacteria, the similar pattern of the bacterial killing property was observed in Gram-positive bacteria.

Keywords : Fe₃O₄, diethylamine, nanoparticle, superparamagnetic, anti-bacteria

1. Introduction

The emergence of global health issues are significantly related to poor environmental hygiene and lack of drug treatment efficacy in clinical management. The improvement of drug treatment efficiency and microbial infection prevention was considered as a part of clinical management goals. Nowadays, the synthesis of composite particles has been promoting a specific strategy in the biotechnological and biomedical field. The utilization of composite in particular magnetic nanoparticles was reported to be widely used in drug delivery, energy storage, and antibacterial agent [1-3]. Superparamagnetic iron oxide nanoparticles are new materials implemented in several biomedical applications particularly against

resistant pathogens [4]. Hence, the synthesis of unique iron oxide especially magnetite (Fe₃O₄) nanoparticles based on their molecular and physical structure is the major concern to enhance the potential properties of these materials in the biophysical study.

Fe₃O₄ nanoparticles become potential particles with a higher capability in the drug-delivery system (DDS), anticancer, antibacterial function, recyclable biocides, and MRI application in clinical diagnosis [5-9]. Moreover, Fe₃O₄ is a stable nanoparticle against oxidation, significantly associated with stable magnetization, biocompatibility agent, and lack of toxicity. In addition, to reduce invasive method in clinical management, nanoparticle applications may offer a novel strategy to heal the specific disease and pathogen clearance in pre and post patient therapy [10]. Magnetic-nanoparticles also provide a novel chance to detect a bacterial resistance to antibiotic treatment [11]. In dealing with the advanced clinical therapies and environmental quality control, the exploration of Fe₃O₄

©The Korean Magnetism Society. All rights reserved.

*Corresponding author: Tel: +62-341-552-125

Fax: +62-341-559-577, e-mail: ahmad.taufiq.fmipa@um.ac.id

nanoparticles synthesized from natural materials with potent antibacterial property and drug delivery capability is required.

To enhance the antibacterial application of the Fe₃O₄ nanoparticles, it is also essential to produce stable Fe₃O₄ ferrofluids with the superparamagnetic character by inexpensive and simple methods. Therefore, we offer the functionalization of natural iron sand to provide the Fe₃O₄ nanoparticles. Furthermore, it is also imperative to first produce the Fe₃O₄ nanoparticles as the main particles in the fluid with small size and high homogeneity. Consequently, the control of the size and uniformity of the Fe₃O₄ nanoparticles become an essential role that should be conducted first. One prospective way that can be performed is by employing an appropriate template in fabricating process of the fluid [12]. Some research groups took efforts to obtain the Fe₃O₄ nanoparticles with small size and excellent uniformity by employing PEG as templates in several types and compositions [13-15]. However, the uniformity of the Fe₃O₄ nanoparticles distribution was not obtained properly. Thus, an alternative template which is based on a soft template should be further explored to achieve Fe₃O₄ nanoparticles in small size and in high homogeneity with superparamagnetic character.

Several previous studies have shown that Fe₃O₄ nanoparticles can be addressed explicitly to inhibit bacterial growth rate. Fe₃O₄@POHABA (poly-N,N'-[(4,5-dihydroxy-1,2-phenylene)bis(methylene)]bisacrylamide) material could decrease Gram-negative, Gram-positive bacteria and fungal cell proliferation rate [1]. The combination of Fe₃O₄ and SiO₂-Ag exhibited antibacterial capabilities of these magnetic hybrid nanocomposites [16]. Furthermore, similar to the previous study, a photothermal bacterial inactivation was reported in the pre-treatment with polydopamine@Fe₃O₄+phenylethanesulfonamide resulting from the inhibition of Hsp70s (70 kilodalton heat shock proteins) [17]. Metal oxide nanoparticles have been claimed as a bacterial growth inhibitor through the enhanced oxygen free radical formation [18]. Iron oxide nanoparticles are predicted to increase bacterial apoptosis due to the higher level of reactive oxygen species (ROS) production and related to the alteration of bacterial cell membrane charge [8]. Importantly, the application of Fe₃O₄ nanoparticles improved lysozyme releasing process resulted in the decrease of bacterial growth at physiological temperature [19]. Even though some previous studies have been conducted to justify the fundamental property of Fe₃O₄ in microbial control, however, there is no information whether the different soft template of Fe₃O₄ synthesis affects the microbial growth rate. Therefore, the

application of natural Fe₃O₄ with different synthesis pattern can be considered as the potential nanoparticles on pathogen population growth control.

In this work, we propose the use of diethylamine as a soft template in synthesizing the Fe₃O₄ nanoparticles from natural iron sand with superparamagnetic behavior. Moreover, the structural, particle size, chemical bonding, superparamagnetic properties, and antibacterial performances are also discussed comprehensively.

2. Experimental Methods

Diethylamine template was utilized to conduct the synthesis of Fe₃O₄ nanoparticles by using a simple co-precipitation method. The magnetite powders were extracted from natural iron sand taken from East Java, Indonesia. The extracting process was set by following our previous works [20, 21]. The magnetite powders extracted from iron sand were then reacted with hydrochloric acid (HCl 12.1 M) using a magnetic stirrer at a room temperature according to our previous works [22-24]. After the solution was formed, the diethylamine was added dropwise with five serial variations of 0 %, 8.3 %, 16.7 %, 25 %, and 33.3 % in volume and followed by dropping slowly of ammonium hydroxide (NH₄OH 6.5 M). The samples with the five compositions of diethylamine were respectively coded by FD1, FD2, FD3, FD4, and FD5. Moreover, the precipitate was washed with deionized water and ethanol and then followed by the filtering process. To obtain the Fe₃O₄ ferrofluids, the Fe₃O₄ particles were reacted by TMAH and dispersed in water. Meanwhile, to obtain the Fe₃O₄ in powders, the samples were then annealed at 100 °C. Finally, the Fe₃O₄ particles were characterized by means of X-ray Diffractometer (XRD), Fourier Transforms Infrared (FTIR) spectroscopy, Brunauer-Emmet-Teller (BET) surface area analyzer, and Superconducting Quantum Interference Device (SQUID) magnetometer.

The XRD experiment was conducted to investigate the phase purity, crystal structure, crystallite size, and lattice parameter of the samples. The XRD data were obtained from the diffractometer with Cu-K α radiation on 40 kV and 35 mA. The FTIR characterization of electromagnetic radiation in the range of 4000-400 cm⁻¹ was performed to study the functional groups of the samples. The BET characterization was also employed to calculate the surface area and the size of the magnetic particles. Moreover, a magnetic measurement of SQUID magnetometer was also conducted to investigate the superparamagnetic character of the Fe₃O₄ nanoparticles.

The growth rate assay of Fe₃O₄ nanoparticles was performed using *E. coli* (Gram-negative bacteria) and *B.*

subtilis (Gram-positive bacteria). In this work, the growth rate is defined as the number of colony formation of Gram-positive and Gram-negative bacteria in agar plate. Both of microbes were obtained from LIPI (Indonesian Science Research Center, Jakarta Indonesia) and pre-cultured within liquid Mueller Hinton agar (Merck Millipore) with bacterial broth dilution method. Next, 500 μL of bacterial samples were diluted with 500 μL magnetite dispersion. One hundred microliters of the dilution samples were used and cultivated in Mueller-Hinton agar plate for the antimicrobial test. The positive control group was treated with chloramphenicol, while the placebo group was prepared without antimicrobial treatment. All of the experimental plates were incubated for 24 hours at 37 $^{\circ}\text{C}$. Fe_3O_4 nanoparticles used soft templates with five serial concentrations in this test. The growth inhibitory activity/cell death stimulation of Fe_3O_4 was calculated by colony formation measurement/Quebec colony counter.

3. Results and Discussion

Figure 1 presents the XRD patterns of the Fe_3O_4 particles mediated by diethylamine prepared by a simple co-precipitation method. Based on the figure, it can be seen that all samples present similar diffraction patterns to the Fe_3O_4 nanoparticles in the literature [25-27]. Qualitatively, the XRD patterns of all samples also refer to the XRD pattern of the Fe_3O_4 with ICSD No. 30860 in a single phase. It means that a variation of the diethylamine as a template does not influence the crystallite phase of the Fe_3O_4 nanoparticles. Moreover, to investigate the crystal structures of the samples in more detail, the quantitative

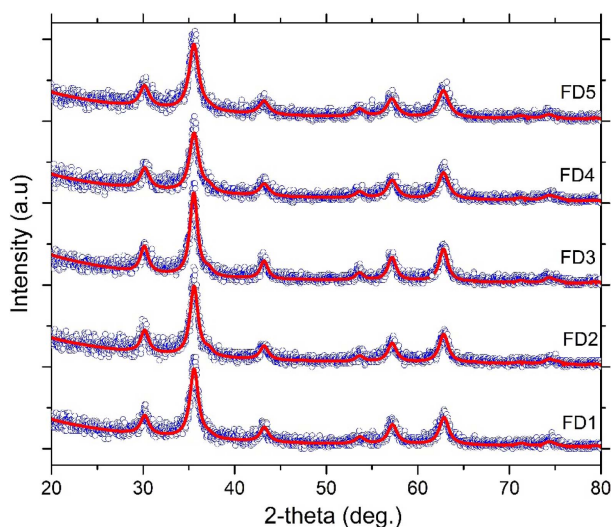


Fig. 1. (Color online) X-ray Diffraction patterns (blue circle) and Rietveld refinement plots (red solid line) of the Fe_3O_4 particles mediated by diethylamine from iron sand.

analysis by using refinement technique is explained in the following discussion.

Based on the results of the refinement analysis using a *Rietica* program with the ICSD as a structural reference, all samples constructed a crystal structure of inverse spinel of Fe_3O_4 . In this structure, all prepared samples have a crystal cubic structure with lattice parameters of $a = b = c$ and crystal volume of $V = a \times b \times c$ [28]. In such structure, the iron ions centered in octahedral and tetrahedral sites are surrounded respectively by six and four oxygen ions. The value of goodness of fit (*GoF*) and profile factor (R_p) represents that the ICSD model is appropriate to fit the XRD data of the samples. In this experiment, the value of the lattice parameters tends to be constant in the range of about 8.361-8.367 \AA as shown in Table 1. These results are also similar to the results as reported in the literature [22-24].

The particle size (D) was determined by using Debye-Scherrer's formula as shown in the following equation [29].

$$D = \frac{K\lambda}{\beta \cos \theta} \quad (1)$$

where θ is the Bragg angle, β is the excessive line broadening which is expressed by the full width at half maximum, K is constant, and λ is the X-ray wavelength.

The data analysis shows that all samples have a particle size of a nanometric size that is lower than 10 nm. The results are also in agreement with the particle size of the Fe_3O_4 investigated by means of synchrotron small-angle X-ray scattering (SAXS) as reported in our previous works [21, 22]. Furthermore, in our previous work, it was reported that the Fe_3O_4 nanoparticles with different sizes were obtained by XRD data and were comparable with the results of HR-TEM and small-angle neutron scattering [23]. The results of data analysis of BET characterization are summarized in Table 1, indicating high surface area value in the range of about 170-617 m^2/g . The trends of the surface area values are in line with the trend of the

Table 1. Crystallite size, lattice parameter, and surface area of the Fe_3O_4 nanoparticles mediated by diethylamine from iron sand.

Sample	GoF	R_p	Crystallite size (nm)	Lattice parameter (\AA)	Surface area (m^2/g)
FD1	0.57	16.25	8.62	8.361	183.6
FD2	0.60	16.62	8.94	8.362	193.8
FD3	0.58	16.33	9.91	8.362	169.7
FD4	0.58	16.58	7.78	8.367	173.2
FD5	0.57	16.00	7.31	8.365	616.8

crystallite size calculated by Debye Scherer's equation from the XRD data. In general, the concentration of diethylamine does not significantly affect the crystal structure of the Fe₃O₄ nanoparticles. However, the increasing of the diethylamine concentration tends to reduce the crystallite size of the Fe₃O₄ nanoparticles. It means that the diethylamine plays an essential role in inhibiting the growth of the Fe₃O₄ nanoparticles by surface capsulation process. Moreover, the diethylamine as a template also increases the nucleation of the Fe₃O₄ nanoparticles. Interestingly, the sample with the highest diethylamine template composition, *i.e.* FD5 has the biggest surface area of 616.8 m²/g corresponding to the smallest particle size which becomes the best candidate for an antibacterial agent for the Gram-negative bacteria. It means that the diethylamine works efficiently as an appropriate template for synthesizing the Fe₃O₄ nanoparticles. Generally, diethylamine has a particular function to prevent the growth of the nanoparticles to control the size of the Fe₃O₄ nanoparticles.

The functional group of the Fe₃O₄ nanoparticles was characterized using the infrared spectrometer by electromagnetic radiation in the range of 4000-400 cm⁻¹. Based on Fig. 3, the Fe₃O₄ nanoparticles have the absorption peaks at 420 and 582 cm⁻¹ which associated with functional groups of Fe³⁺-O²⁻ and Fe²⁺-O²⁻ in the spinel structure [30, 31]. These peaks correspond to the XRD data analysis as shown in the above discussion. The vibration of reminder H₂O on the surface of the Fe₃O₄ nanoparticles is detected in the absorption bands of approximately 1630 and 3430 cm⁻¹ [32]. Meanwhile, the peak near 1360 cm⁻¹ belongs to Fe-O bonding in tetrahedral position. Furthermore, the weak peak at the spectrum of 2315 cm⁻¹ is believed from CO₂ from the atmosphere [33]. Interestingly, the figure exhibits the absence of functional groups of diethylamine in the FTIR spectra. Based on the literature,

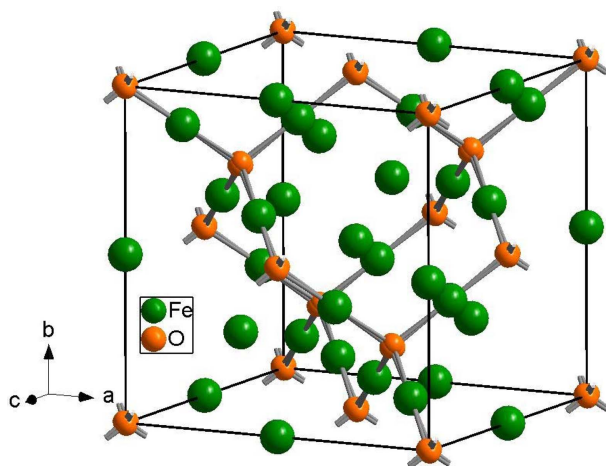


Fig. 2. (Color online) Crystal structure of the Fe₃O₄ particles.

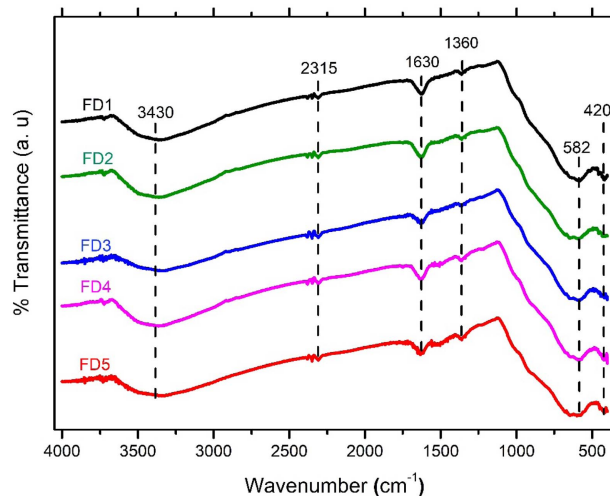


Fig. 3. (Color online) FTIR spectra of the Fe₃O₄ nanoparticles mediated by diethylamine from iron sand.

the functional groups of the diethylamine appear at 733 cm⁻¹ (N-H), 1143 cm⁻¹ (C-N) and 3288 cm⁻¹ (N-H) [29]. It means that the annealing process of the precipitated materials at 100 °C could easily remove the diethylamine content. Therefore, the diethylamine plays an essential role as a soft template in preparing the Fe₃O₄ nanoparticles. Moreover, the use of diethylamine in preparing the Fe₃O₄ nanoparticles does not contaminate the purity of the magnetic particles. To ensure that this experiment has successfully produced Fe₃O₄ nanoparticles with the superparamagnetic character, the magnetic characterization will be discussed in the following section.

Figure 4 shows magnetic properties of the Fe₃O₄ nanoparticles dispersed in water. The magnetization experi-

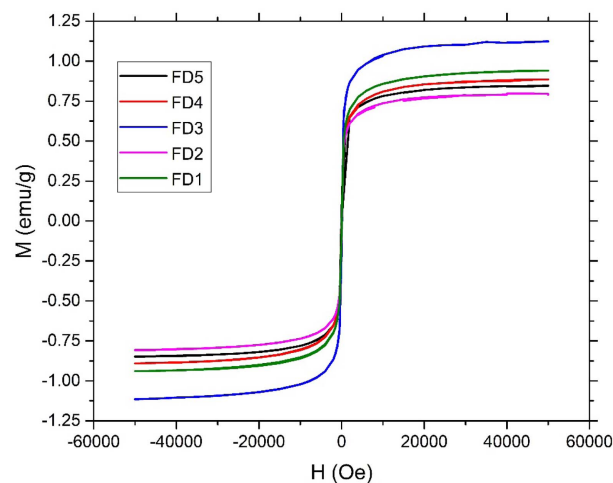


Fig. 4. (Color online) Magnetization curves of the Fe₃O₄ fer-rofluids mediated by diethylamine from iron sand.

ment was conducted by sweeping the magnetic field (H) from -5 T to 5 T at a room temperature. The magnetization (M) of all samples increased and decreased sharply from 0 to 5 T and from 0 to -5 T, respectively. Moreover, the magnetization curve formed S shape with the coercivity force and a remanent magnetization that is almost negligible. Mathematically, the magnetization curves follow the Langevin function as described comprehensively in the literature [34]. In the superparamagnetic state, without the external magnetic field, the Fe_3O_4 nanoparticles have no residual magnetism with almost zero coercivity. These properties become strong physical evidence that the Fe_3O_4 nanoparticles prepared in this experiment have an excellent behavior as being superparamagnetic [35]. In our previous work [22], the Fe_3O_4 nanoparticles with the diameter size of about 8 nm present a superparamagnetic character based on the M-H curve and FC-ZFC data. In such data, the blocking temperature appears at 270 K indicating that the Fe_3O_4 nanoparticles have a superparamagnetic feature at a room temperature. Theoretically, without any influences of an external magnetic field, the magnetic moment of superparamagnetic material has random orientation. On the other hand, under an external magnetic field, the magnetic moment of the material is easily oriented by following the direction of the external field.

Based on the magnetization curves, the saturation magnetization is in the range of 0.6 - 1.2 emu/g. The FD3 sample has the highest saturation magnetization with the value of approximately 1.1 emu/g. It is predicted that this phenomenon occurs because the FD3 sample has the highest particle size compared to the other samples as shown in the above XRD and BET data analysis. However, for a global data, the saturation magnetization of the samples does not follow a linear trend with the particle size. Theoretically, despite the saturation magnetization of the Fe_3O_4 particles is contributed by net magnetic moment of iron ions in the tetrahedral and octahedral sites, the literature points out that the magnetization is also contributed by many factors such as the size of primary and secondary particles, particle shapes, spin disorder, and metallic ion arrangements [22, 36]. From the magnetization curves, it can be inferred that the natural iron sand has been successfully utilized in producing high purity magnetic nanoparticles with the superparamagnetic character using a soft-template technique. Furthermore, to enhance the functionalization of the prepared magnetic nanoparticles, the investigation of their antibacterial performance is also presented in the following segment.

Our study has attempted to explore the potential antibacterial activity of the Fe_3O_4 nanoparticles in the fluids

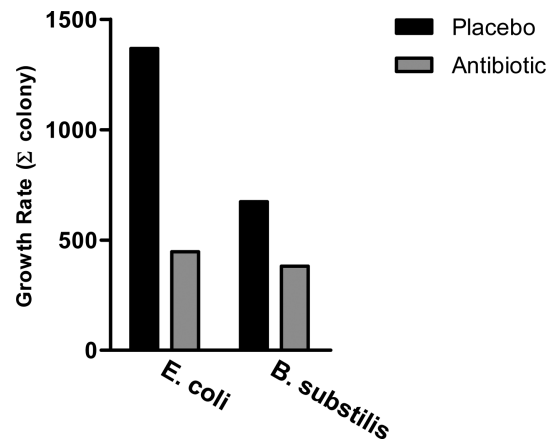


Fig. 5. The growth rate of placebo as negative control and positive control group with antibiotic treatment.

synthesized from natural resources with soft-template synthesis model. The preliminary laboratory observation was done by growing the Gram-positive (*B. subtilis*) and Gram-negative (*E. coli*) bacteria on medium with and without an antibiotic treatment as presented in Fig. 5. The figure shows that the bacterial growth rate in the negative control group (placebo) significantly higher than the positive control group with an antibiotic treatment in both gram bacteria. The pre-administration of antibacterial agent (chloramphenicol) significantly reduced the number of colony formation (bacterial growth rate in agar plate). Theoretically, antibiotic treatment acts to prevent the bacterial growth rate by decreasing cell proliferation. Furthermore, to clarify that the prepared Fe_3O_4 nanoparticles play an essential role in inhibiting the bacterial growth rate, we have treated both Gram bacterial with five serial samples as shown in Fig. 6.

The antibacterial activity of the Fe_3O_4 nanoparticles obtained from local resources showed a significant outcome to a bacterial growth rate. The pre-administration of

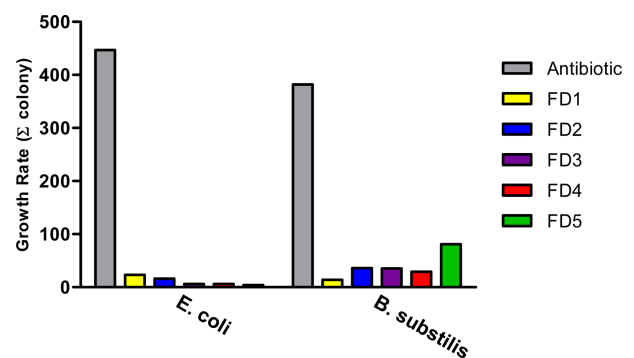


Fig. 6. (Color online) The Fe_3O_4 nanoparticles treatment decreased the growth rate of Gram-positive and Gram-negative bacteria.

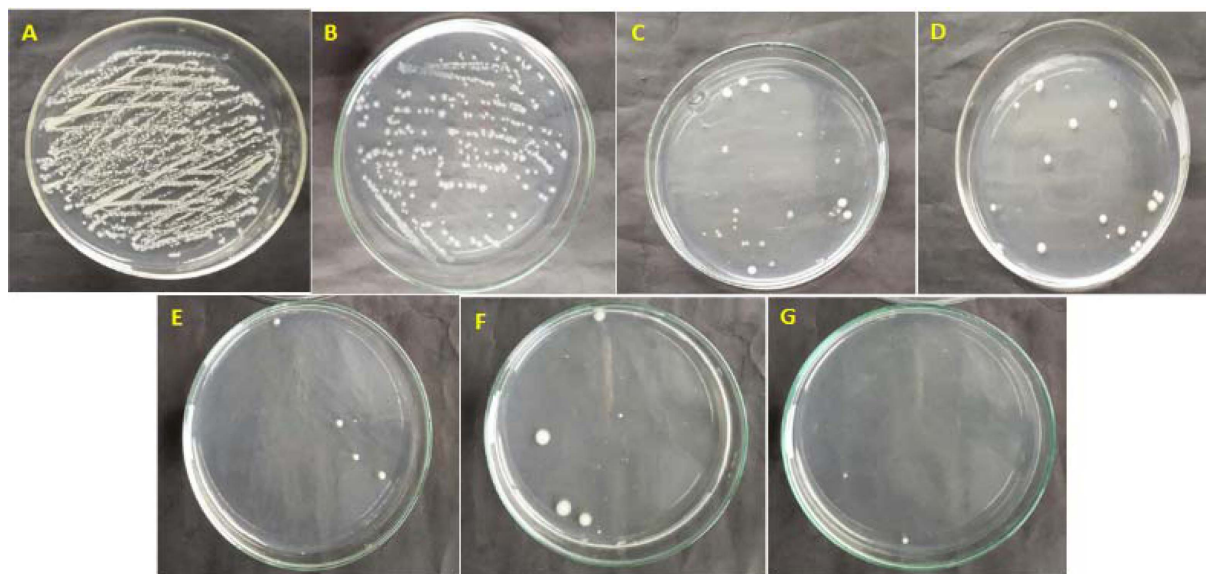


Fig. 7. (Color online) Antimicrobial test of the Fe₃O₄ ferrofluids at Gram-negative bacteria; A. Control (*E. coli*); B. Positive control (*E. coli* + chloramphenicol); C-G. Experimental group (*E. coli* treated with five serial soft templates for the Fe₃O₄ nanoparticles synthesis). C, D, E, F, and G refer to the respective samples of FD1, FD2, FD3, FD4, and FD5.

Fe₃O₄ nanoparticles significantly reduced the colony formation compared to the control group as shown in Fig. 6. In particular, for the Gram-negative bacteria growth rate observation, pretreatment with Fe₃O₄ nanoparticles significantly declined the colony formation compared to placebo and positive control group as shown in Fig. 6. Also, in line with this data, the similar pattern of the bacterial killing property was observed in Gram-positive

bacteria as presented in Figs. 7-8. However, the consistency of Fe₃O₄ nanoparticles to decrease pathogen proliferation rate was significantly different in Gram-negative bacteria compared to Gram-positive bacteria.

The decreasing number of colony forming unit bacteria in this work presented that the potential antibacterial occurs from the Fe₃O₄ nanoparticles. One important reason of this phenomenon is that the magnetic nanoparticles can

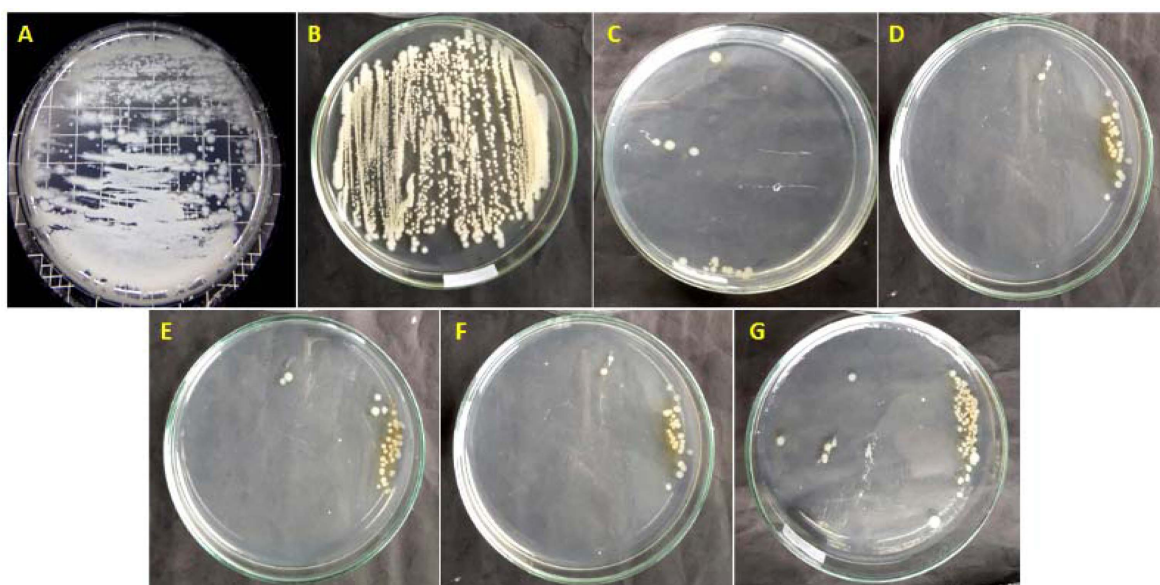


Fig. 8. (Color online) Antimicrobial test of the Fe₃O₄ ferrofluids at Gram-positive bacteria; A. Control (*B. subtilis*); B. Positive control (*B. subtilis* + chloramphenicol); C-G. Experimental group (*B. subtilis* treated by five serial soft templates for the Fe₃O₄ nanoparticles synthesis). C, D, E, F, and G refer to the respective samples of FD1, FD2, FD3, FD4, and FD5.

deactivate the synthesis of essential complex proteins on bacteria or can be employed as protein synthesis inhibitor especially for protein transport, adhesion, receptor, ion channel, cytoskeleton, enzyme [37], and on ribosome, cell wall, cytoplasmic membrane, lipid biosynthesis enzyme, transcription factor, and deoxyribonucleic acid (DNA) replication [38]. Conversely, the effect of the Fe₃O₄ nanoparticles on bacteria occurs through a molecular process such as binding between the Fe₃O₄ nanoparticles wall and cell wall, releasing of metallic ions, or formation of reactive oxygen species [2]. In particular, the Fe₃O₄ nanoparticles could produce reactive oxygen species leading to the inhibition of bacterial proliferation in both Gram-positive and Gram-negative bacteria. Moreover, the electromagnetic attraction between the microbes and the Fe₃O₄ nanoparticles becomes possible mechanism originated from positive and negative charges from the Fe₃O₄ and the microbes, respectively [9]. Therefore, it is believed that the Fe₃O₄ nanoparticles have a better performance in inhibiting the Gram-negative bacterial growth (*E. coli*) than Gram-positive bacterial growth (*B. subtilis*). Based on the electromagnetic concept, the interaction between positive and negative charges is attractive while positive and positive charges are repulsive. According to the results of this work, a further investigation of antibacterial activity of the Fe₃O₄ nanoparticles by applying external magnetic and electric fields becomes an important and challenging research to be conducted.

4. Conclusion

Diethylamine as a soft template was successfully employed to produce Fe₃O₄ nanoparticles with high purity from natural iron sand. All samples were crystallized in the inverse spinel structure as Fe₃O₄ and sized in the nanometric scale below 10 nm. The functional groups of all samples exhibited a high purity of Fe₃O₄ particles without any impurities. Moreover, the magnetic characterization of the Fe₃O₄ nanoparticles in the fluids presented superparamagnetic materials. The Fe₃O₄ ferrofluids presented an essential outcome to pathogen growth rate served as an excellent antibacterial agent. Compared to control group, the pre-administration of bacterial stock solution (*E. coli* and *B. subtilis*) with the Fe₃O₄ significantly reduced the colony formation.

Acknowledgment

The authors would like to appreciate the KEMENRISTEKDIKTI RI through Universitas Negeri Malang for giving research grant for AT. The authors also

would like to thank D. Yuliantika for preparing antibacterial characterization.

References

- [1] Z. Zhang, D. Xing, X. Zhao, and X. Han, Environ. Sci. Pollut. Res. **24**, 19011 (2017).
- [2] S. Stankic, S. Suman, F. Haque, and J. Vidic, J. Nanobiotechnology **14**, 73 (2016).
- [3] G. Mirabello, J. J. M. Lenders, and N. A. J. M. Somerdijk, Chem. Soc. Rev. **45**, 5085 (2016).
- [4] L. M. Tung, N. X. Cong, L. T. Huy, N. T. Lan, V. N. Phan, N. Q. Hoa, L. K. Vinh, N. V. Thinh, L. T. Tai, and K. Mølhave, J. Nanosci. Nanotechnol. **16**, 5902 (2016).
- [5] J. Chen, W. Zhang, M. Zhang, Z. Guo, H. Wang, M. He, P. Xu, J. Zhou, Z. Liu, and Q. Chen, Nanoscale **7**, 12542 (2015).
- [6] P. Gong, H. Li, X. He, K. Wang, J. Hu, W. Tan, S. Zhang, and X. Yang, Nanotechnology **18**, 285604 (2007).
- [7] B. Liu, C. Li, Y. Chen, Y. Zhang, Z. Hou, S. Huang, and J. Lin, Nanoscale **7**, 1839 (2015).
- [8] S. F. Situ and A. C. S. Samia, ACS Appl. Mater. Interfaces **6**, 20154 (2014).
- [9] Y. T. Prabhu, K. V. Rao, B. S. Kumari, V. S. S. Kumar, and T. Pavani, Int. Nano Lett. **5**, 85 (2015).
- [10] M. Hashim, S. E. Shirsath, S. S. Meena, R. K. Kotnala, A. Parveen, A. S. Roy, S. Kumar, P. Bhatt, and R. Kumar, J. Magn. Magn. Mater. **341**, 148 (2013).
- [11] T. A. Cowger, Y. Yang, D. E. Rink, T. Todd, H. Chen, Y. Shen, Y. Yan, and J. Xie, Bioconjug. Chem. **28**, 890 (2017).
- [12] B. Huang, M. Cao, F. Nie, H. Huang, and C. Hu, Def. Technol. **9**, 59 (2013).
- [13] M. Anbarasu, M. Anandan, E. Chinnasamy, V. Gopinath, and K. Balamurugan, Acta. A. Mol. Biomol. Spectrosc. **135**, 536 (2015).
- [14] E. A. Setiadi, P. Sebayang, M. Ginting, A. Y. Sari, C. Kurniawan, C. S. Saragih, and P. Simamora, J. Phys. Conf. Ser. **776**, 012020 (2016).
- [15] Y. Junejo, A. Baykal, and H. Sözeri, Cent. Eur. J. Chem. **11**, 1527 (2013).
- [16] S.-S. Chen, H. Xu, H.-J. Xu, G.-J. Yu, X.-L. Gong, Q.-L. Fang, K.C.-F. Leung, S.-H. Xuan, and Q.-R. Xiong, Dalton Trans. **44**, 9140 (2015).
- [17] D. Liu, L. Ma, L. Liu, L. Wang, Y. Liu, Q. Jia, Q. Guo, G. Zhang, and J. Zhou, ACS Appl. Mater. Interfaces **8**, 24455 (2016).
- [18] T. Gordon, B. Perlstein, O. Houbara, I. Felner, E. Banin, and S. Margel, Colloids Surf. Physicochem. Eng. Asp. **374**, 1 (2011).
- [19] E. Yu, I. Galiana, R. Martínez-Máñez, P. Stroeve, M. D. Marcos, E. Aznar, F. Sancenón, J. R. Murguía, and P. Amorós, Colloids Surf. B Biointerfaces **135**, 652 (2015).
- [20] Sunaryono, A. Taufiq, Munaji, B. Indarto, Triwikantoro,

- M. Zainuri, and Darminto, AIP Conf. Proc. **1555**, 53 (2013).
- [21] Sunaryono, A. Taufiq, E. G. R. Putra, A. Okazawa, I. Watanabe, N. Kojima, S. Rugmai, S. Soontaranon, M. Zainuri, Triwikantoro, S. Pratapa, and Darminto, Nano **11**, 1650027 (2015).
- [22] A. Taufiq, Sunaryono, N. Hidayat, A. Hidayat, E. G. R. Putra, A. Okazawa, I. Watanabe, N. Kojima, S. Pratapa, and Darminto, Nano **12**, 1750110 (2017).
- [23] A. Taufiq, Sunaryono, E. G. Rachman Putra, A. Okazawa, I. Watanabe, N. Kojima, S. Pratapa, and Darminto, J. Supercond. Nov. Magn. **28**, 2855 (2015).
- [24] A. Taufiq, Sunaryono, E. G. Rachman Putra, S. Pratapa, and Darminto, Mater. Sci. Forum **827**, 213 (2015).
- [25] A. Sahu, P. S. Badhe, R. Adivarekar, M. R. Ladole, and A. B. Pandit, Biotechnol. Rep. **12**, 13 (2016).
- [26] X. Cui, S. Belo, D. Krüger, Y. Yan, R. T. M. de Rosales, M. Jauregui-Osoro, H. Ye, S. Su, D. Mathe, N. Kovács, I. Horváth, M. Semjani, K. Sunassee, K. Szigeti, M. A. Green, and P. J. Blower, Biomaterials **35**, 5840 (2014).
- [27] S. Khodabakhshi, B. Karami, K. Eskandari, S. J. Hoseini, and H. Nasrabadi, Arab. J. Chem. **10**, S3907 (2017).
- [28] W. D. Callister and D. G. Rethwisch, Materials science and engineering: an introduction, 8th ed, John Wiley & Sons, Hoboken, NJ, (2010).
- [29] S. Ahmad, U. Riaz, A. Kaushik, and J. Alam, J. Inorg. Organomet. Polym. Mater. **19**, 355 (2009).
- [30] M. Ramalakshmi, P. Shakkthivel, M. Sundrarajan, and S. M. Chen, Mater. Res. Bull. **48**, 2758 (2013).
- [31] A. Kaushik, R. Khan, P. R. Solanki, P. Pandey, J. Alam, S. Ahmad, and B. D. Malhotra, Biosens. Bioelectron **24**, 676 (2008).
- [32] M. Ma, Y. Zhang, W. Yu, H. Shen, H. Zhang, and N. Gu, Colloids Surf. Physicochem. Eng. Asp. **212**, 219 (2003).
- [33] A. Gatelytė, D. Jasaitis, A. Beganskienė, and A. Kareiva, Mater. Sci. **17**, 302 (2011).
- [34] B. D. Cullity and C. D. Graham, Introduction to Magnetic Materials, 2nd edition, Wiley-IEEE Press, Hoboken, N.J., (2008).
- [35] R. Rameshbabu, R. Ramesh, S. Kanagesan, A. Karthigeyan, and S. Ponnusamy, J. Supercond. Nov. Magn. **27**, 1499 (2014).
- [36] G. F. Goya, T. S. Berquó, F. C. Fonseca, and M. P. Morales, J. Appl. Phys. **94**, 3520 (2003).
- [37] M. Wink, Medicines **2**, 251 (2015).
- [38] M. T. Madigan, Brock biology of microorganisms, 13th ed, San Francisco, (2012).